Experimental Characterization of Cascaded Vapor Chambers for Spreading of Non-Uniform Heat Loads

Soumya Bandyopadhyay
School of Mechanical Engineering
Purdue University
West Lafayette, USA
bandyop0@purdue.edu

Norawish Lohitnavy
School of Mechanical Engineering
Purdue University
West Lafayette, USA
nlohitna@purdue.edu

Amy M. Marconnet
School of Mechanical Engineering
Purdue University
West Lafayette, USA
amarconn@purdue.edu

Justin A. Weibel
School of Mechanical Engineering
Purdue University
West Lafayette, USA
jaweibel@purdue.edu

Abstract*— Thermal management of heterogeneous electronic devices relies on spreading high local heat fluxes in the package lid. The use of intra-lid vapor chambers is an attractive approach if they can be designed for the thermal management of a large total heat load simultaneous with localized high-flux hotspots. Conventional vapor chambers, having a single vapor core, require thick evaporator wicks to avoid the capillary limit at high total power, but these thick evaporator wicks impose a large conduction resistance to hotspots. The recently proposed cascaded multi-core vapor chamber (CMVC) concept consists of a bottom-tier comprising multiple vapor cores that can each diffuse high heat flux hotspots before they reach the top tier, which acts as a conventional single-core vapor chamber. The current study experimentally investigates the use of cascaded vapor chambers for heat spreading of a non-uniform heat load to illustrate this design rationale. The thermal resistance of a solid copper benchmark, a conventional vapor chamber, and a cascade of two vapor chambers are compared for non-uniform heat input. Experiments are performed by interfacing the heat spreaders with a central heater generating the peak heat flux surrounded by a film heater that produces a lower heat flux background power; the other side of the spreaders is interfaced to a cold plate to provide a controlled boundary condition. The results demonstrate that the cascaded vapor chambers offer a notable reduction in thermal resistance relative to the conventional vapor chamber. The enhancement in performance is attributed to the local dampening of the peak heat fluxes at a low thermal resistance, thereby reducing the total thermal resistance of the cascaded vapor chambers relative to the standalone vapor chamber. This result reveals that cascades of vapor chambers have the potential to perform better than conventional vapor chambers through attenuation of hotspots at a low thermal resistance.

***Keywords*—** heterogeneous integration, electronics packaging, vapor chamber, hotspot, non-uniform

Nomenclature

Q	heat input
R	thermal resistance
T	temperature
x	length

Subscripts

bg	background
cp	cold plate
evap	evaporator
pk	peak
sp	spreader

I. Introduction

State-of-the-art heterogeneous electronic packages include multifarious functional components within the same package. These packages often have highly non-uniform power maps requiring thermal management of a large total heat load simultaneously with high-density hotspots. Internal resistances to heat flow out of the package can result in excessive temperatures that significantly affect device reliability. Current typical thermal management strategies rely on spreading high local heat fluxes by conduction in the package lid, ultimately dissipating the total heat load using a mounted heat sink [1]. Embedding passive intra-lid heat spreaders is a potential approach to mitigate excessive temperatures by effectively diffusing the local hotspots within the package.

In the context of passive heat spreaders, vapor chambers have been established as a reliable candidate for the thermal management of electronic devices [2]. Vapor chambers consist of a sealed chamber lined on the inside walls by porous wick structures that generate a capillary pressure head to passively circulate an internal working fluid. Liquid is continuously pumped to the location of heat input, where it evaporates and it absorbs heat. The vapor flows throughout the inner core and rejects heat by condensation over a larger area, where the heat is then dissipated to a heat sink or cold plate. The reliable passive operation of vapor chambers renders them suitable candidates for integration into high-power heterogeneous packages.

Many recent investigations have focused on designing and characterizing new vapor chamber architectures that change the internal layout and wick structure to affect the fluid return to the evaporator to improve performance [3]. Hwang et al. [4] experimentally characterized a vapor chamber architecture comprising multiple wick columns connecting the evaporator and condenser of the architecture. Koukoravas et al. [5] experimentally characterized a vapor chamber comprising a wettability patterned condenser, using a resistive heater to provide a uniform heat flux of ~100 W/cm^2 over ~ 1 cm^2. Chen et al. [6] conducted experiments with a vapor chamber containing radial multi-artery reentrant microchannels under a uniform heat flux generated by a light-emitting diode (LED) module. Wang et al. [7] fabricated and experimentally tested copper-water vapor chambers comprising grooved wick structures under a uniform heat flux ranging up to ~40 W/cm^2

over 9 cm^2, generated by cartridge heaters inserted inside a copper heater block. Liu et al. [8] experimentally characterized miniaturized silicon vapor chambers under a uniform heat flux greater than 60 W/cm^2, provided by a serpentine heater over a 3.2 mm x 3.2 mm area.

Several investigations take an alternative approach of focusing on the design of the evaporator wick placed directly over the heat source to increase the maximum heat flux dissipation. A common approach is the experimental characterization of hybrid or micro-patterned wick structures designed for maintaining low surface temperatures while dissipating high heat fluxes over large areas. Hybrid evaporator wicks experimentally characterized by Ju et al. [9] were capable of dissipating heat fluxes exceeding 375 W/cm^2 over a 4 cm^2 evaporator area. Weibel et al. [10] experimentally demonstrated grid-patterned sintered wick structures to dissipate heat fluxes greater than 500 W/cm^2 over a 0.25 cm^2 evaporator area. Semenic et al. [11] demonstrated the dissipation of 520 W/cm^2 from a ~0.3 cm^2 evaporator area using thin biporous sintered wicks. Sudhakar et al. [12,13] characterized a two-layer evaporator wick, which dissipates high uniform heat fluxes of 512 W/cm^2 from relatively large heat input areas of 1 cm^2. Separately, many studies have developed and experimentally characterized evaporator wicks intended for dissipating extremely high heat fluxes concentrated in smaller hotspot areas, including power densities of 770 W/cm^2 [14] and 938 W/cm^2 [15] over 0.04 cm^2 areas using biporous carbon nanotube wicks, as well as >1200 W/cm^2 over ~0.006 cm^2 areas using copper inverse opal wicks [16].

A notable omission from past work is that both changes in the vapor chamber architectures and changes to the internal evaporator wick designs have not been developed for (or characterized under) conditions having both background power at a low heat flux and high heat flux hotspots, despite the importance and prevalence of this power map. To address this gap, our recent work introduced [17] and performed a parametric optimization [18] of the concept of a cascaded multi-core vapor chamber (CMVC) to spread a total background heat load from the entire die area, while also minimizing the temperature rise associated with high heat flux hotspots. The CMVC comprises a bottom-tier core having an array of many tiny vapor cores over the die footprint that can each dampen high heat flux hotspots at a low thermal resistance before they pass through to the single vapor core that functions as a conventional vapor chamber in the top tier.

The present study aims to experimentally illustrate this design rationale for the use of cascaded vapor chambers by demonstrating that they offer a lower net thermal resistance compared to a conventional single-core vapor chamber. This is achieved by characterizing the thermal resistance of the copper spreader benchmark, a standalone vapor chamber, and the same vapor chamber but with a smaller footprint buffer vapor chamber placed below. The experimental facility, testing procedures, and data reduction methods are first introduced. The measured temperatures are used to compare the total thermal resistance of the heat spreaders and report the trends as a function of the peak and background heat fluxes.

II. Experimental Methods

An experimental facility is used to characterize the thermal resistance of a copper spreader, a conventional vapor chamber, and cascaded vapor chambers subjected to a non-uniform heat input. The experiments are performed using a copper spreader (see Figure 1(b)) having dimensions 90 mm × 90 mm × 3 mm, as well as commercially available vapor chambers having dimensions 90 mm × 90 mm × 3 mm (Wakefield Vette) and 30 mm × 30 mm × 3 mm (Novark). The cascaded vapor chambers (Figure 1(d)) comprise a buffer vapor chamber (30 mm x 30 mm x 3 mm) interfacing a top vapor chamber (90 mm x 90 mm x 3 mm; Figure 1(c)) with a gap pad. The non-uniform power map (see Figure 1(a)) has a peak heat load (Q_{pk}) over 100 mm^2 (denoted by red). This centrally located heat load is surrounded by a background heat flux area (denoted by pink), having an edge length (x_{bg}) of 22.5 mm, that generates a uniform total background power (Q_{bg}).

A. Experimental facility

The experimental facility (see Figure 2), briefly reviewed here, was previously reported in Ref. [17] to evaluate the thermal resistance of heat spreaders at differing operating temperatures and under a uniform heat load. The centers of the heat spreaders are soldered to the top 10 mm × 10 mm surface of an insulated oxygen-free copper block heated by a cartridge heater. The facility is modified for the current study to generate a non-uniform power map. Custom-designed polyimide film heaters (Tramonto Circuits) are affixed to the underside of the heat spreaders, surrounding the central copper heater block, using pressure-sensitive adhesive. The top surface of the heat spreader interfaces with the bottom surface of a cold plate (Aavid Thermalloy) via a thermal gap pad (Tflex™ HD700, Laird). For the cascaded vapor chambers, the top vapor chamber is interfaced with the buffer vapor chamber below using the same type of gap pad. Deionized water is pumped through the cold plate (insulated on top with fiberglass) with a refrigerating bath circulator (RW-0525G, Lab Companion) that controls the temperature.

B. Testing procedure

Experiments are performed with the copper spreader, conventional vapor chamber, and cascaded vapor chambers for different background heat fluxes at a given peak heat flux. For all experiments, the liquid temperature in the refrigerating bath circulator is maintained at 70 °C. The peak heat flux (q''_{pk}) is first set to a constant value ranging from 18.5 W/cm^2 to 52.2 W/cm^2. At every peak heat flux level, the background heat flux (q''_{bg}) is then increased from 0 W/cm^2 to two different heat fluxes of 5.5 W/cm^2 and then 7.4 W/cm^2. The peak and background heat fluxes are controlled using separate power sources. For each combination of peak and background heat flux, steady-state data are recorded for the respective heat spreaders once the system temperatures become constant (a change less than ~0.01 °C/s), which takes ~30 min between successive heat fluxes. This set of test points is selected to reveal the dependence of the performance of the heat spreaders on both the peak and background heat fluxes.

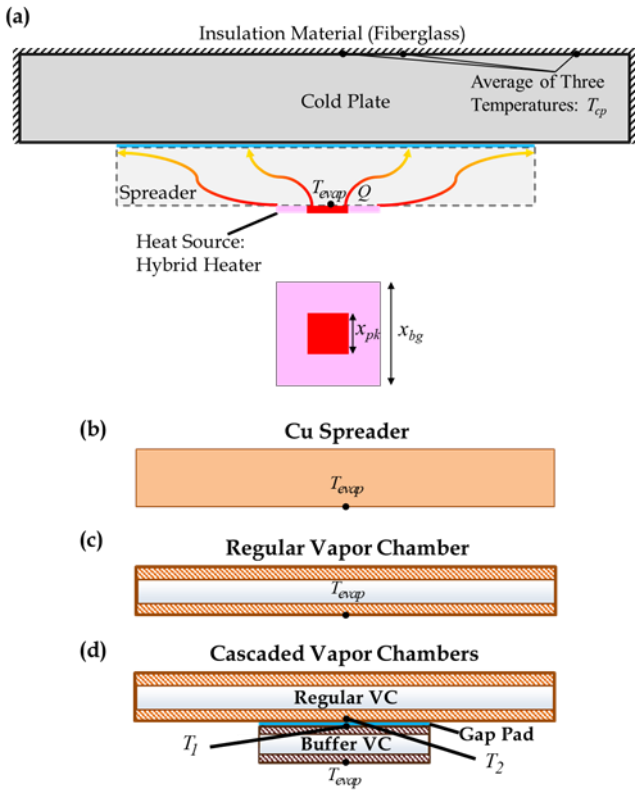

Fig. 1 (a) Schematic cross-section of the heat spreader boundary conditions in the experiment. Top view of the representative power map footprint comprising a peak (red) heat load of side length x_{pk}, centered on the background (pink) heat flux of side length x_{bg}. Schematic cross-sections of the (b) solid copper, (c) regular vapor chamber, and (d) cascaded vapor chambers test cases.

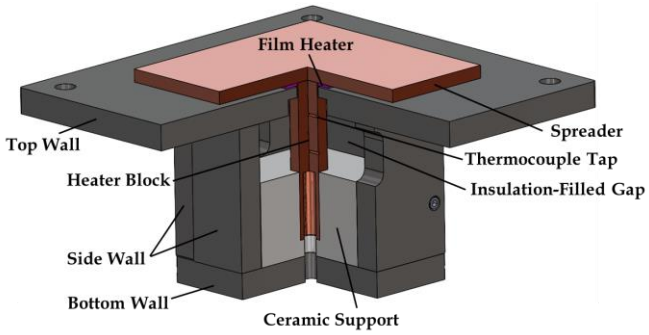

Fig. 2 Isometric cut view of the heater block testbed for experimental characterization of a heat spreader. A copper heater block insulated by ceramic and PEEK provides a uniform heat flux to the base of the heat spreader soldered atop. Thermocouples are used to measure the temperature gradient along the centerline of the copper block for estimating the heat input to the spreader. The film heater (pink) is fixed at the base of the heat spreader surrounding the heater block.

C. Data reduction

All thermocouples used for temperature measurement are ice-point-referenced (TRCIII, Omega) and calibrated using a dry-block calibrator (Jupiter 4852 Advanced, Isotech). The temperature gradient, measured from a linear fit to a rake of four thermocouples inside the copper heater block, is employed to estimate the peak heat flux to a given heat spreader. Uncertainty in the measured peak heat flux is estimated to be less than 4% based on the calibrated uncertainties in the temperature (± 0.2 °C) and the location of the measurements. The voltage across the film heater is measured using a data acquisition system and the background heat flux is subsequently estimated using the electrical resistance of the film heater. The uncertainty in the background heat load is estimated from the uncertainties in the measured voltage and the electrical resistance of the film heater. Heat losses from the film heater are within the uncertainty bounds reported in the results. All uncertainties related to calculating the peak heat load from the heater block are calculated as described in Ref. [19].

The maximum temperature at the base (T_{evap}) of the heat spreaders is measured by laying a thermocouple (± 0.6 °C) into a shallow groove fabricated on the bottom surface. The temperature at the top surface of the cold plate (T_{cp}) is estimated from an average of three thermocouple measurements distributed over the surface. The thermal resistance for the copper and the conventional vapor chamber is then directly calculated based on the difference between the base and cold plate temperatures and the peak heat load (Q_{pk}), as:

$$R_{evap,cp} = \frac{T_{evap} - T_{cp}}{Q_{pk}} \quad . \tag{1}$$

For the experiment with cascaded vapor chambers, the temperature drop across the thickness of the thermal interface material is directly measured by placing thermocouples in grooves on the condenser (T_1) of the buffer vapor chamber and the bottom of the regular vapor chamber (T_2). The concept of a cascaded multi-core vapor chamber comprises both the top and bottom tier, sharing a common copper wall at the interface. Hence, the total thermal resistance of the cascaded vapor chambers is then estimated by subtracting the temperature drop across the thermal interface material from the total temperature difference given in Equation 1.

III. Results

Experiments with the solid copper benchmark, the conventional vapor chamber, and the cascaded vapor chambers are used to estimate, compare, and discuss the relative thermal resistances for uniform and then non-uniform heat input.

A. Uniform heat load

Figure 3(a) shows the measured spreader thermal resistance ($R_{evap,cp}$) as a function of the peak flux in absence of background heat load. The measured spreader thermal resistance for all of the heat spreaders is observed to remain nearly constant (with a slight reduction for the regular vapor chamber) with an increase in the peak heat flux. The invariance of the spreader thermal resistance for different levels of heat flux is characteristic of a solid heat spreader and therefore is expected for the copper case. For the regular vapor chamber and the cascaded vapor chambers, this is attributed to the dominance of the conduction resistance across the evaporator wicks relative to the vapor core thermal resistance, as previously demonstrated in Ref. [18]. The results show that the conventional vapor chamber performs worse (higher resistance) relative to the copper spreader. While this performance relative to the benchmark is highly specific to the given boundary conditions and design of the commercial vapor chamber, much more notably, we observe that the

introduction of a buffer vapor chamber significantly lowers the total thermal resistance of the cascaded vapor chambers relative to the standalone vapor chamber. This intriguing result is a key proof-of-principle that the use of a cascade of vapor chambers can provide a thermal resistance advantage by locally spreading heat from a hotspot that is much smaller than the available condenser footprint area.

B. Non-uniform power map

The maximum total thermal resistance of the cascaded vapor chambers is compared to the conventional vapor chamber and the solid copper benchmark with an increasing background heat flux at multiple different peak heat fluxes in Figures 3(b), (c), and (d). In our experiments, the temperature drop across the thermal interface material accounts for approximately 50% of the difference in the maximum evaporator temperature and the average cold plate temperature. For any given peak heat flux, the maximum spreader thermal resistance universally increases as the background heat flux is increased. This is attributed to the normalization of the thermal resistance by the peak heat load, as there is a necessary increase in the maximum temperature at the base of the heat spreader due to the increased total heat load, even though the peak heat flux is held constant.

More importantly, comparing the thermal resistance across the heat spreader types for each peak heat flux, the thermal resistance is the largest for the conventional vapor chamber. As in the uniform heating cases, the cascaded vapor chambers offer a notable reduction in the thermal resistance relative to the conventional vapor chamber for every peak heat flux. For a peak heat flux of 18.7 W/cm^2, the thermal resistance of the cascaded vapor chambers was 26 – 35 % lower than the standalone regular vapor chamber over the range of background heat fluxes. Similarly, when the peak heat flux is 33.6 W/cm^2 or 50.6 W/cm^2, there was a 31 - 34% or 14 – 19 % reduction in the thermal resistance, respectively. The buffer vapor chamber attenuates the peak heat flux while simultaneously managing the background power at a low thermal resistance. The local dampening of the peak before it enters the top vapor chamber also attenuates its thermal resistance so significantly that the total thermal resistance of the stack of vapor chambers is lower than the standalone conventional vapor chamber. This promising result provides evidence that the use of cascaded vapor chambers, and thereby the CMVC concept, is a viable strategy for simultaneously spreading peak heat flux and a background power at a reduced thermal resistance.

IV. Conclusion

Experiments demonstrate the use of a cascaded of vapor chambers under a non-uniform heat load to reduce the spreading thermal resistance compared to a single vapor chamber. A solid copper benchmark, conventional vapor chamber, and the cascaded vapor chambers are interfaced with a central heater generating the peak heat flux surrounded by a film heater that produces a background power at a lower heat flux. The trends in the measured thermal resistance of the heat spreaders are recorded for a range of peak and background heat fluxes. For the given range of experimental parameters, the thermal resistance of the copper spreader was similar to the cascaded vapor chamber within the uncertainty limits. The results demonstrate that cascaded vapor chambers offer a significant maximum reduction in thermal resistance by 35% relative to the conventional vapor chamber for a given non-uniform power map.

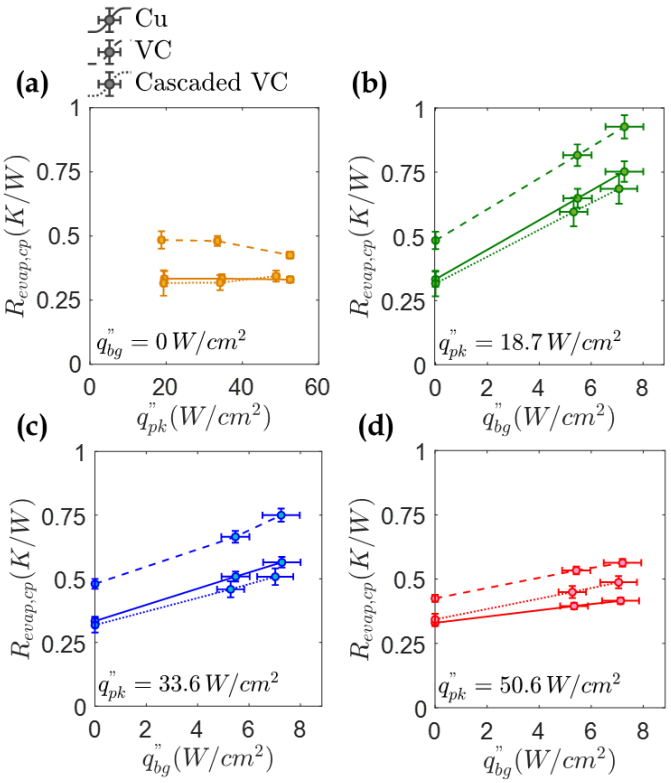

Fig. 3 Comparison of the heat spreader thermal resistance for the solid copper benchmark (Cu; solid line), conventional single-core vapor chambers (VC; dashed line), and cascaded vapor chambers (dotted line). Panel (a) shows the variation of the heat spreader thermal resistance as a function of the peak heat flux when there is no background heat load. Panels (b), (c), and (d) illustrate the variation of the heat spreader thermal resistance as a function of the background heat flux for different hot spot heat fluxes.

This performance enhancement is attributed to the local dampening of the peak heat fluxes by the vapor core of the buffer vapor chamber, at a low thermal resistance, thereby reducing the total thermal resistance of the cascaded vapor chambers relative to the standalone vapor chamber. This result illustrates the principal design rationale behind the cascaded multi-core vapor chamber (CMVC) concept for heat spreading from a non-uniform power map, as it reveals that a cascade of vapor chambers can outperform a conventional vapor chamber through attenuation of peak heat fluxes at a low thermal resistance.

Acknowledgment

This work was supported by Semiconductor Research Corporation (SRC), as a part of the Global Research Collaboration (GRC) Program on Packaging (PKG; Science Director, Dr. John Oakley) in the Center for Heterogeneous Integration Research on Packaging (CHIRP). We are thankful to the SRC liaisons, Dr. Rajiv Mongia, Dr. Feras Eid, Dr. Kamal Sikka, and Dr. Anil Yuksel, for their discussion and input on the work.

REFERENCES

[1] IEEE Heterogeneous Integration Roadmap: Chapter 3 (https://eps.ieee.org/images/files/HIR_2020/ch03_iot.pdf)

[2] Bulut, M., Kandlikar, S.G., and Sozbir, N., 2019. A review of vapor chambers. Heat Transfer Engineering, **40**(19), pp.1551-1573.

[3] Weibel, J.A. and Garimella, S.V., 2013. Recent advances in vapor chamber transport characterization for high-heat-flux applications. Advances in Heat Transfer, **45**, pp. 209-301.

[4] Hwang, G.S., Nam, Y., Fleming, E., Dussinger, P., Ju, Y.S., and Kaviany, M., 2010. Multi-artery heat pipe spreader: experiment. International Journal of Heat and Mass Transfer, **53**(13-14), pp.2662-2669.

[5] Koukoravas, T.P., Damoulakis, G., and Megaridis, C.M., 2020. Experimental investigation of a vapor chamber featuring wettability-patterned surfaces. Applied Thermal Engineering, **178**, p.115522.

[6] Chen, L., Deng, D., Huang, Q., Xu, X. and Xie, Y., 2020. Development and thermal performance of a vapor chamber with multi-artery reentrant microchannels for high-power LED. Applied Thermal Engineering, **166**, p.114686.

[7] Wang, M., Cui, W., and Hou, Y., 2019. Thermal spreading resistance of grooved vapor chamber heat spreader. Applied Thermal Engineering, **153**, pp.361-368.

[8] Liu, T., Dunham, M.T., Jung, K.W., Chen, B., Asheghi, M., and Goodson, K.E., 2020. Characterization and thermal modeling of a miniature silicon vapor chamber for die-level heat redistribution. International Journal of Heat and Mass Transfer, **152**, p.119569.

[9] Ju, Y.S., Kaviany, M., Nam, Y., Sharratt, S., Hwang, G.S., Catton, I., Fleming, E., and Dussinger, P., 2013. Planar vapor chamber with hybrid evaporator wicks for the thermal management of high-heat-flux and high-power optoelectronic devices. International Journal of Heat and Mass Transfer, **60,** pp.163-169.

[10] Weibel, J.A. and Garimella, S.V., 2012. Visualization of vapor formation regimes during capillary-fed boiling in sintered-powder heat pipe wicks. International Journal of Heat and Mass Transfer, **55**(13-14), pp.3498-3510.

[11] Semenic, T. and Catton, I., 2009. Experimental study of biporous wicks for high heat flux applications. International Journal of Heat and Mass Transfer, **52**(21-22), pp.5113-5121.

[12] Sudhakar, S., Weibel, J.A., Zhou, F., Dede, E.M., and Garimella, S.V., 2019. Area-scalable high-heat-flux dissipation at low thermal resistance using a capillary-fed two-layer evaporator wick. International Journal of Heat and Mass Transfer, **135**, pp.1346-1356.

[13] Sudhakar, S., Weibel, J.A., Zhou, F., Dede, E.M., and Garimella, S.V., 2020. The role of vapor venting and liquid feeding on the dryout limit of two-layer evaporator wicks. International Journal of Heat and Mass Transfer, **148**, p.119063.

[14] Cai, Q. and Bhunia, A., 2012. High heat flux phase change on porous carbon nanotube structures. International Journal of Heat and Mass Transfer, **55**(21-22), pp.5544-5551.

[15] Cai, Q. and Chen, Y.C., 2012. Investigations of biporous wick structure dryout. Journal of Heat Transfer, **134**(2), p.021503.

[16] Palko, J.W., Zhang, C., Wilbur, J.D., Dusseault, T.J., Asheghi, M., Goodson, K.E., and Santiago, J.G., 2015. Approaching the limits of two-phase boiling heat transfer: High heat flux and low superheat. Applied Physics Letters, **107**(25), p.253903.

[17] Bandyopadhyay, S., Marconnet, A.M. and Weibel, J.A., 2020. A Cascaded Multi-Core Vapor Chamber for Intra-Lid Heat Spreading in Heterogeneous Packages. 19th IEEE Intersociety Conference on Thermal and Thermomechanical Phenomena in Electronic Systems (ITherm), pp. 963-969.

[18] Bandyopadhyay, S., Marconnet, A.M. and Weibel, J.A., 2020. Cascaded Multi-Core Vapor Chambers for Intra-Package Spreading of High Power, Heterogeneous Heat Loads. (In Review).

[19] Sarangi, S., Weibel, J.A., and Garimella, S.V., 2015. Effect of particle size on surface-coating enhancement of pool boiling heat transfer. International Journal of Heat and Mass Transfer, **81**, pp.103-113.